Journal of the European Ceramic Society 23 (2003) 203–212

www.elsevier.com/locate/jeurceramsoc

Peculiarities of the pyroelectric effect and of the dielectric properties in Bi-doped $Pb(Zr_{0.95}Ti_{0.05})O_3$ ceramics

Z. Ujma*, J. Hańderek

Institute of Physics, University of Silesia, ul. Uniwersytecka 4, 40-007 Katowice, Poland

Received 15 November 2001; accepted 25 May 2002

Abstract

Unusual behaviour of the pyroelectric effect and some peculiarities of the dielectric characteristics in the vicinity of AFE↔FE phase transitions in Bi-doped $Pb(Zr_{0.95}Ti_{0.05})O_3$ ceramics are confirmed. Two pyroelectric peaks are found both on heating and cooling through this phase transition. They occur at temperatures, which depend on the strength of the DC field, and on other conditions of the pre-poling procedure. The internal bias electric field associated with the metastable space charge polarisation is considered to be the reason for the observed peculiarities in the pyroelectric effect and dielectric properties.

Keywords: Dielectric properties; Ferroelectric properties; Phase transitions; Pyroelectric effect; PZT

1. Introduction

The Zr-rich $Pb(Zr_{0.95}Ti_{0.05})O_3$ ceramics, denoted as PZT-95/5, are intensively studied due to many as yet unsolved problems relating to their specific properties resulting from the coexistence of two ferroelectric phases (low and high temperature $F_{R(LT)}$ and $F_{R(HT)}$ — both of rhombohedral symmetry) with a neighbouring antiferroelectric one (of orthorhombic symmetry A_O).[1–14]

Dielectric characteristics from the temperature range of phase transitions in the undoped and La-, Nb-doped PZT-95/5 ceramics are shown in Fig. 1 (according to Refs. [12–14]). Strong broadening of AFE-FE phase transition and especially the big effect of its thermal hysteresis are the most typical properties of these ceramics. Unusual behaviour of the pyroelectric effect was also ascertained in the vicinity of this phase transition.[12] Small anomalies in dielectric characteristics are associated with $F_{R(LT)}$–$F_{R(HT)}$ phase transition. The phase transition between $F_{R(HT)}$ and paraelectric (PE) phases is related to a greater extent to the normal, first order phase transition (Fig. 1). The steep phase boundaries separating the low temperature phases in the temperature-composition phase diagram of the PZT system, stabilisation of individual phases and dielectric and pyroelectric characteristics are strongly dependent on substitutions of various elements for Pb or/and Zr/Ti. In case of the PZT-95/5 ceramics the influence of Nb and La dopants have most often been investigated.[3–5,9–11] Some results of such investigations were also reported in our previous papers.[12–15] Authors all agree that substitution of Nb for Zr stabilises the rhombohedral ferroelectric phases.[9] Opinions differ, however, on the influence of substitution of La for Pb. Some authors maintain that antiferroelectricity is favoured by this substitution.[2] Our results, reported in Ref.[13] point to the widening of the intermediate FE phase(s) with increase of La content. Literature available differs as to many other details concerning the phase diagrams of the PZT system. This also includes dielectric and pyroelectric properties. The influence of many modifiers is still of great interest and the subject of intensive studies.

The mentioned above peculiarities of dielectric and pyroelectric characteristics in the temperature region of AFE-FE-PE phase transitions may also be expected in the Bi-doped PZT-95/5 ceramics. The Bi_2O_3 dopant improves, on one hand, the sinterability and microstructure of the studied ceramics and, on the other hand, Bi^{3+} ions substituted for Pb create specific defects, thus changing the balance of electron-hole cur-

* Corresponding author. Tel.: +48-32-588211x1134; fax: +48-32-588431.

E-mail address: ujma@us.edu.pl (Z. Ujma).

0955-2219/02/$ - see front matter
PII: S0955-2219(02)00180-2

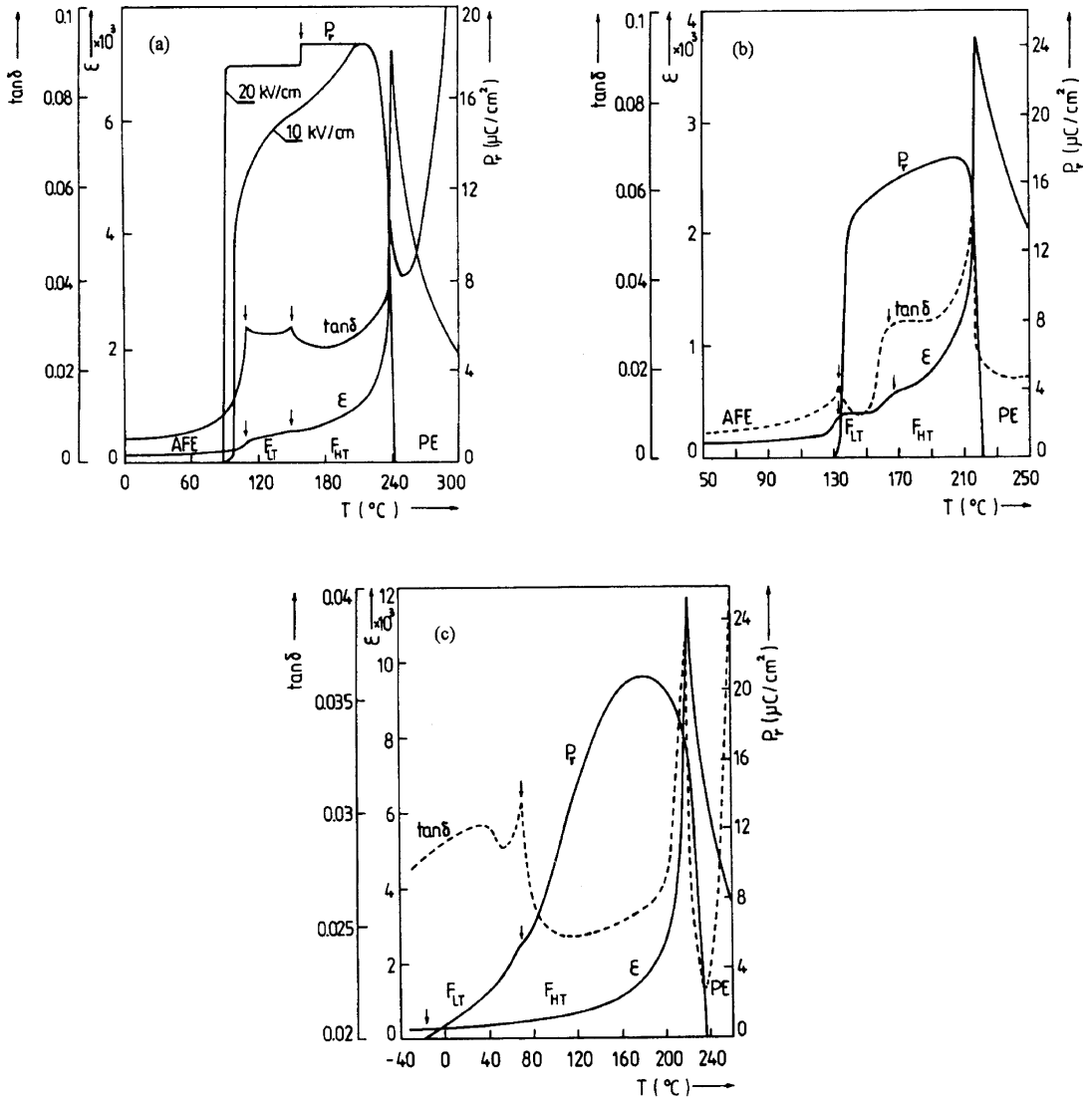

Fig. 1. Comparison of the dielectric constant (ϵ), the dielectric loss (tanδ) and the remanent polarisation (P_r) as functions of temperature for the undoped (a) and doped with 1 mol% of La_2O_3 (b) and 1 mol% of Nb_2O_5 (c) PZT 95/5 ceramics (see Ref. 15).

rent carriers. These space charges, as shown below, influence both the phase transition temperatures as well as the electric and pyroelectric properties in their vicinities. The possibility of controlling the modifications of these properties is of both cognitive and application importance.

2. Preparation and grain structure of the studied ceramics

The $Pb(Zr_{0.95}Ti_{0.05})O_3$ ceramics doped with 0.5; 1; 1.5 and 2 mol% of Bi_2O_3 (that is 1, 2, 3 and 4 at.% of Bi substituted for Pb) were prepared using a conventional method of sintering. Thermal synthesis of blended and pressed mixture of PbO, ZrO_2, TiO_2 and Bi_2O_3 oxides was carried out at 950 °C for the period of 3 h. Crumbled, milled and sieved materials were pressed again in the form of cylinders and then sintered at 1100 °C for 3 h. This procedure was repeated again before final sintering at 1260 °C for 12 h. The two sintering processes were performed in a double crucible with interior $PbO + ZrO_2$ atmosphere to prevent sublimation of PbO at high sintering temperature. The Archimedes displacement method with distilled water was employed to evaluate sample density. Sample bulk densities ranged from 7.30 to 7.75 g/cm^3 for ceramics with 1 and 4 at.% of Bi, respectively. Porosity of these ceramics was less than 8%.

The scanning electron microscope JSM-5410 with energy dispersion X-ray spectrometer (EDS) was used for investigation of the grain structure and to control the distribution of individual elements within the grains. Images of the grain structure on the fracture surface of PZT-95/5 ceramics doped with 1 and 4 at.% of Bi are shown in Fig. 2(a) and (b), respectively. A distribution

of the grain size was observed in all the studied ceramics. The increase of Bi concentration causes decrease of the average grain size from 12 to 7 μm. The EDS analysis indicates a fairly homogeneous distribution of all the elements (Pb, Zr, Ti, O and Bi) throughout the grains.

3. Measurements of spontaneous polarisation

The ferroelectric nature of the intermediate phase(s) between antiferroelectric (A_O) and paraelectric (P_C) ones was proved by hysteresis loops measurements. The computerised automatic measuring system was used for the investigation of the hysteresis loops within the temperature range between A_O–F_R and F_R–P_C transformations. The system made it possible to determine the values of remanent spontaneous polarisation (P_r) on the basis of the observed saturated hysteresis loops. The samples of 0.2 mm thickness were used for the measurements of hysteresis loops, in order to obtain characteristics of P_r versus temperature. These measurements were performed in an electric field of frequency 50 Hz and strength 10 kV/cm. An example of the $P_r(T)$ and coercive field $E_C(T)$ curves, obtained in this way on the heating-cooling cycle, is shown in Fig. 3. A steep increase in the $P_r(T)$ curve appeared during heating on passing through the temperature of about 90 °C, whereas a steep decrease occurred in the vicinity of Curie temperature (T_C). The change in $P_r(T)$ on cooling through this temperature is also typical of the first order FE–PE phase transition. In the temperature range $\sim 100 \div \sim 40$ °C the course of the $P_r(T)$ curves differ markedly on cooling through the $F_R \rightarrow A_O$ phase transition. The P_r decreases slowly in this temperature range during cooling, contrary to its change on heating. Consequently, A_O–F_R phase transition shows an exceptionally big thermal hysteresis effect. This transition has a strongly broadened character, in particular on cooling. Repetition of measurements with electric field of strength 20 kV/cm gives results similar to those shown in Fig. 3, both on heating and on cooling.

Comparison of $P_r(T)$ curves, obtained on heating, for all the studied ceramics is shown in Fig. 4. The $P_r(T)$ curves are relatively similar for the PZT-95/5 ceramics doped with 1–4 at.% of Bi. Tendency of the increase of maximal values of P_r with the increase in Bi content is however noticeable. The $P_r(T)$ curve for the ceramics with the smallest Bi content differ considerably from the other curves shown in Fig. 4. The P_r values are much smaller and the additional local change in the $P_r(T)$ curve can be detected in the vicinity at about 150 °C. This might be a trace of $F_{R(LT)}$–$F_{R(HT)}$ phase transition, observed in undoped PZT-95/5 ceramics exactly at this temperature [Fig. 1(a)].[12]

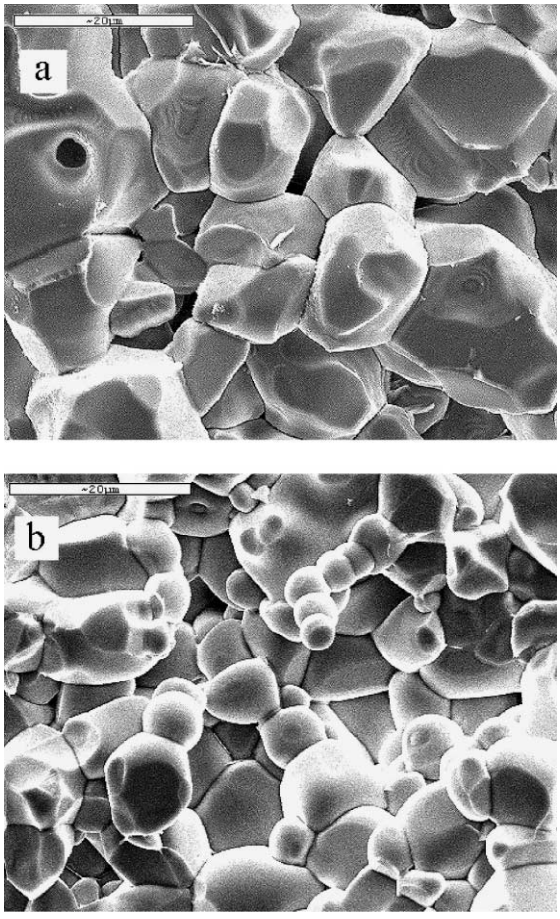

Fig. 2. SEM images of the fracture surface of PZT 95/5 ceramics with 1 at.% (a) and 4 at.% (b) of Bi contents.

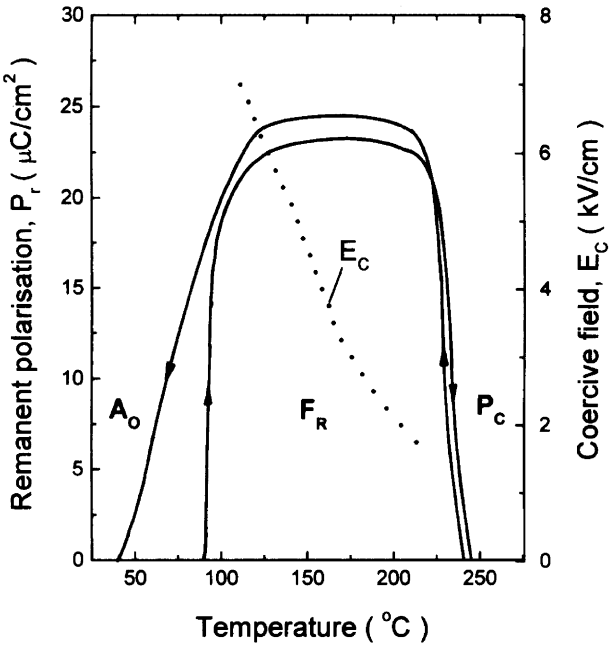

Fig. 3. Remanent polarisation (P_r) on heating and cooling and coercive field (E_C) on heating vs temperature determined from hysteresis loop measurements for PZT 95/5 doped with 2 at.% of Bi.

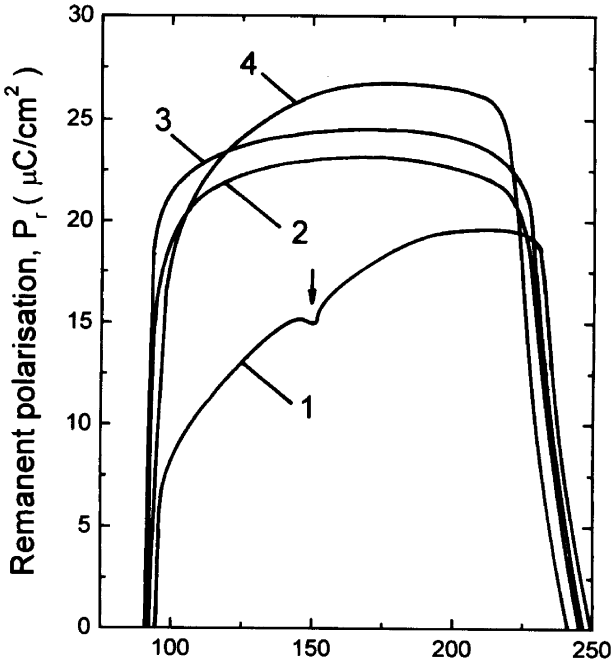

Fig. 4. Remanent polarisation vs temperature obtained on heating for ceramics doped with at.% of Bi shown in the figure.

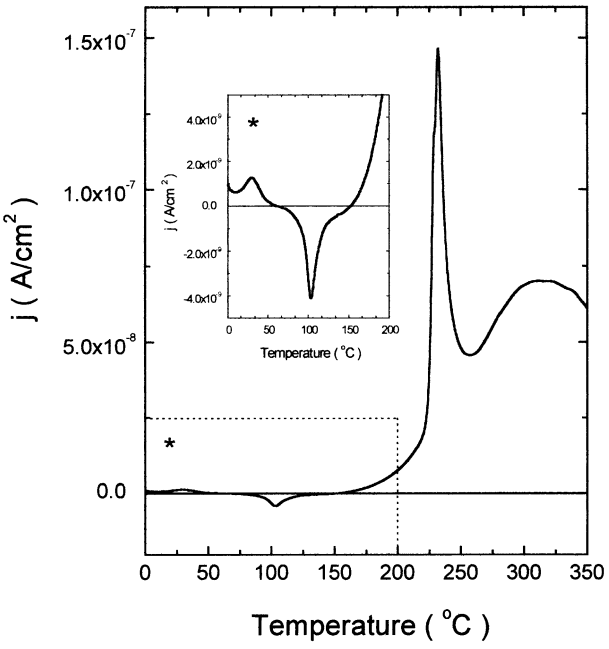

Fig. 5. Pyroelectric and thermally stimulated depolarisation currents vs temperature for ceramics with 2 at.% of Bi, pre-polarised in conditions described in the text.

4. Pyroelectric measurements

Our earlier studies of the pyroelectric effect in the undoped PZT-95/5 ceramics revealed its unusual behaviour in the temperature range of the $A_O \leftrightarrow F_R$ phase transitions.[12] This justified to carry out pyroelectric measurements also for the studied Bi-doped ceramics.

The pyroelectric effect was observed after initial polarisation of these ceramics in DC field of strength 6 kV/cm, applied for 15 min at temperature $T = 250$ °C from the range of PE phase, in one of the experiments carried out. The samples were then cooled for 30 min in the field up to the temperature of −25 °C (within the range of A_O phase) at which the field was switched off. The polarised samples were subsequently heated with a constant temperature rate 5K/min through the A_O–F_R and F_R–P_C phase transition temperatures. For the ceramics with 2 at.% of Bi, pyroelectric peaks associated with appearance and disappearance of spontaneous polarisation in the vicinities of A_O–F_R and F_R–P_C phase transitions are shown in Fig. 5. The pyroelectric peaks from the vicinity of A_O–F_R phase transition are inset in Fig. 5, owing to their small height in comparison with the peak occurring in the vicinity of T_C temperature. The comparison of peaks in the pyroelectric coefficient for all the studied Bi-doped ceramics is shown in Fig. 6(a) and (b), for the vicinities of F_R–P_C and A_O–F_R phase transition temperatures, respectively. The first peaks from the range of T_C temperature are shifted up to about 10 °C towards lower temperature with increase of Bi content [Fig. 6(a)], unlike the peaks accompanying the A_O–F_R phase transition, which are shifted 3–4 °C upwards [Fig. 6(b)].

Additional measurements were carried out in order to elucidate the unusual behaviour mentioned above of the pyroelectric effect in the vicinity of A_O–F_R phase transition and the appearance of an additional peak at lower temperature (inset in Fig. 5). The same pre-polarisation procedure was repeated, but this time, the DC field of strength 6 kV/cm was applied at 175 °C, i.e. within the ferroelectric phase. The sample was then heated through T_C up to 400 °C with simultaneous recording of the pyroelectric current and thermally stimulated depolarisation current (TSDC), appearing in the range of PE phase [Fig. 7(a)]. A sharp peak in the pyroelectric current occurs at T_C. Wide maximum in the TSDC can be seen in the temperature range ~250–375 °C. The sample was then pre-polarised again under the same conditions and then subsequently cooled through $F_R \rightarrow A_O$ phase transition temperature. Two pyroelectric peaks were recorded in this case; one of them, relatively small, at about 15 °C and another one of opposite sign at about 0 °C [Fig. 7(b)].

The following experiment was carried out in order to find the origin of the two peaks in the pyroelectric current, accompanied by phase transition(s) to the AFE state [Fig. 7(b)]. The selected sample of ceramics with 2 at.% of Bi was this time pre-polarised by applying DC field of strength 1, 2, and 6 kV/cm at 250 °C for 15 min and during cooling up to 100 °C. The sample was cooled to −25 °C after each of these procedures, with recording of the pyroelectric current. The recorded pyroelectric peaks are shown in Fig. 8. The smaller

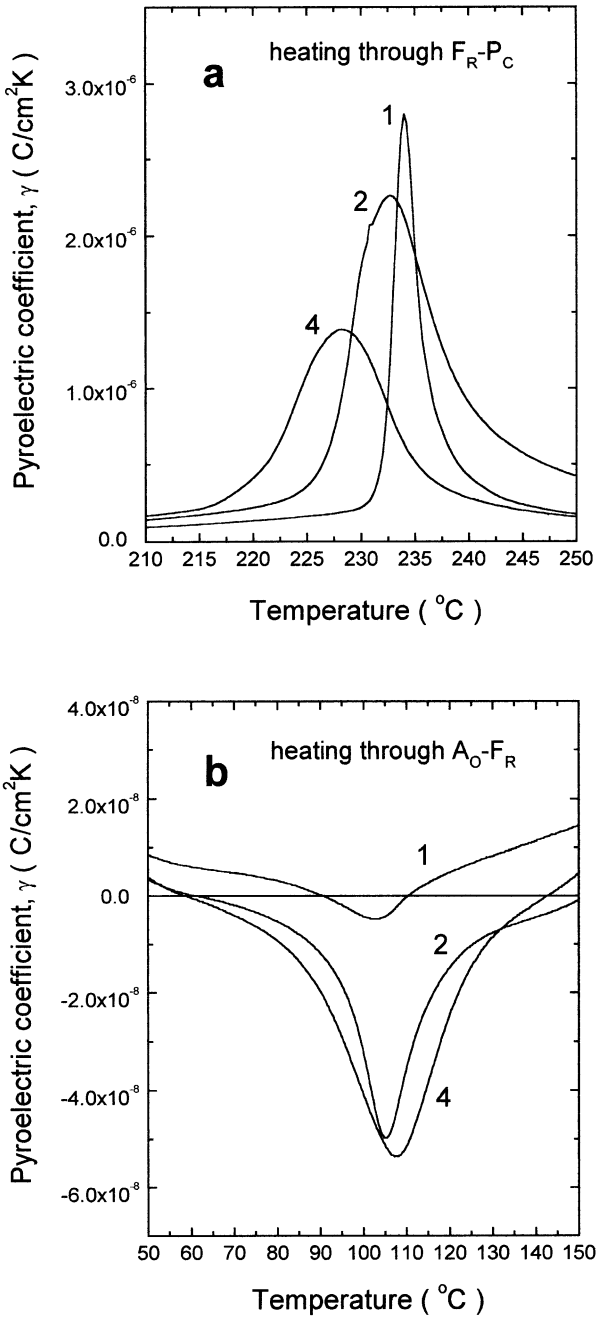

Fig. 6. The pyroelectric coefficient as a function of temperature in the vicinity of $F_R \rightarrow P_C$ (a) and $A_O \rightarrow F_R$ (b) phase transitions for ceramics with at.% shown in the figure.

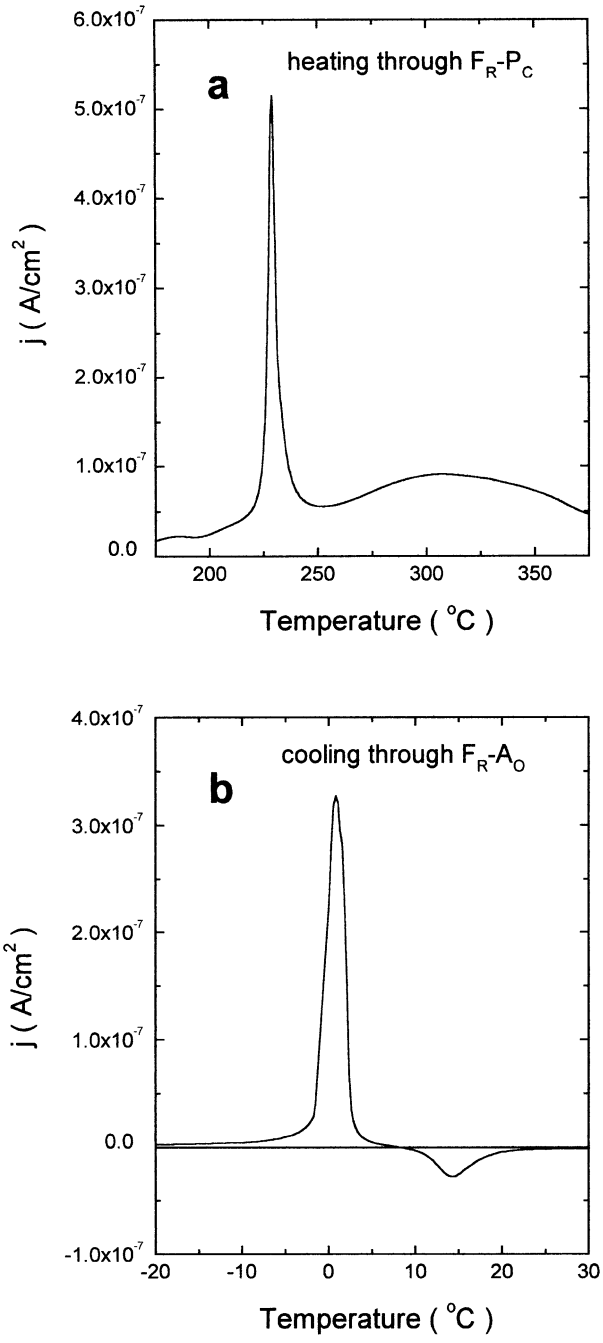

Fig. 7. Pyroelectric and thermally stimulated depolarisation currents vs temperature in the vicinity of $F_R \rightarrow P_C$ (a) and $F_R \rightarrow A_O$ (b) phase transitions for ceramics doped with 2 at.% of Bi, pre-polarised in conditions described in the text.

peaks of negative sign appear at temperatures from the range of 15–13 °C. The other peaks, of positive sign, show also a shift towards lower temperature from ~7 °C to −2 °C with increase of strength of DC field from 1 to 6 kV/cm. Moreover, both kinds of peaks show an increase with rise of strength. Further increase of strength above 6kV/cm did not induce further increase of these peaks.

The peaks of pyroelectric current, recorded for the sample pre-polarised in DC field of 6 kV/cm [Figs. 7(a) and (b) and 8] made it possible to determine the approximate temperature changes of spontaneous polarisation, accompanied by A_O–F_R and F_R–P_C phase transitions. This was done by graphic integration of the pyroelectric current over time. To achieve this the temperature coordinate in Figs. 7 and 8 was converted onto time by taking into account the constant rate of temperature variation while recording the pyroelectric current. The results obtained are shown in Fig. 9 (dashed lines). The

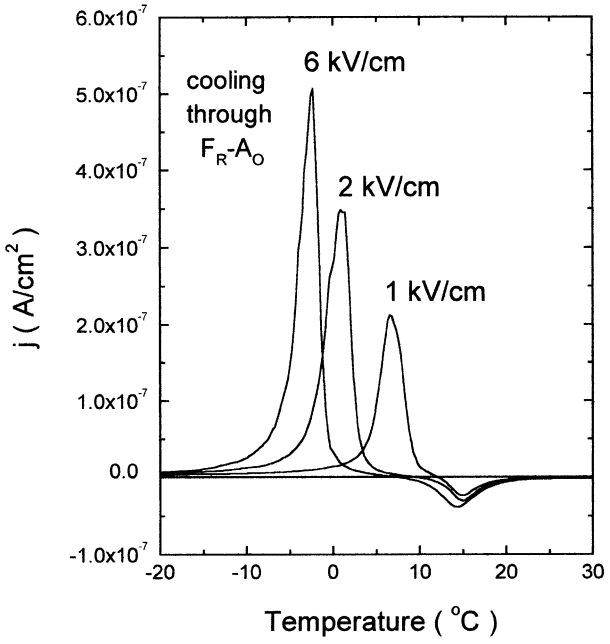

Fig. 8. Pyroelectric current vs temperature for ceramics doped with 2 at.% of Bi, pre-polarised by DC field of strength 1, 2 and 6 kV/cm applied at temperature 250 °C and switched off at 100 °C, and subsequently cooled through $F_R \rightarrow A_O$ phase transition.

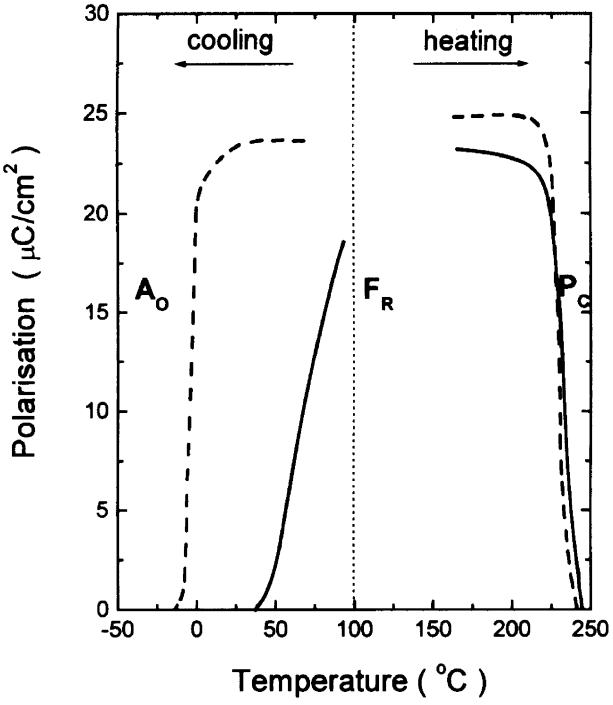

Fig. 9. Comparison of $P_r(T)$ curves determined from hysteresis loop measurements (solid lines) and polarisation vs temperature determined from pyroelectric measurements (dashed lines) in the vicinity of $F_R \rightarrow P_C$ and $F_R > A_O$ phase transitions for ceramics doped with 2 at.% of Bi.

$P_r(T)$ curves determined from the hysteresis loop measurements (Fig. 3) are also shown, for comparison, in Fig. 9 (solid lines). It is worth noting that the $P(T)$ curves, determined by the two mentioned methods show a very similar course and particularly, a conformity of the maximum of P_s ($\sim$25 μC/cm^2). This concerns also, to a certain degree the maximal value of P_s in the vicinity of $F_R \rightarrow A_O$ phase transition. In this case, however, the course of $P(T)$ curves, obtained from hysteresis measurement and from pyroelectric current differs substantially. The $P(T)$ curve, determined from the pyroelectric current is shifted considerably towards lower temperatures in comparison with the $P(T)$ curve, determined from the hysteresis loop measurements. The experiment, whose results are shown in Fig. 8, clearly shows that this shift is caused by the pre-polarisation effect in DC electric field. The temperatures of phase transitions, which can be determined from the measurements of the hysteresis loop and the pyroelectric effect are in fact changed by AC/DC field applied during or before these measurements. In order to find the temperatures of phase transitions, not changed by the measuring conditions dielectric measurements in a weak measuring electric field had to be carried out.

5. Dielectric measurements

Samples of 0.6 mm thickness were used for measurements of the dielectric constant ε′ and of the dissipation factor tanδ as a function of temperature. These measurements were preceded by thermal treatment at about 400 °C in order to cause partial recombination of defects frozen after the sintering process. The strains, caused by mechanical treatment during cutting and polishing, were also removed in this way.

The curves $\varepsilon'(T)$ and $\tan\delta(T)$ measured at 1 kHz frequency of the measuring field on heating and cooling for the ceramics PZT-95/5 doped with 2 at.% of Bi are shown in Fig. 10. A slight anomaly in the $\varepsilon'(T)$ curve, associated the $A_O \rightarrow F_R$ and $F_R \rightarrow A_O$ phase transitions occur at temperatures 113 and 13 °C, respectively—inset in Fig. 10(a). Much clearer symptoms of these phase transitions at the given temperatures are observed in the $\tan\delta(T)$ curves [Fig. 10(b)]. Sharp maxima in $\varepsilon'(T)$ curves and local minima in the $\tan\delta(T)$ curves occur at $F_R \leftrightarrow P_C$ phase transition temperatures 233 and 230 °C on heating and cooling, respectively. Other ceramics, with 1, 3 and 4 at.% of Bi, show similar behaviour with slightly different phase transition temperatures.

A computerised, automatic system was used to measure the dielectric constant at several frequencies of the measuring field as a function of temperature. These measurements were carried out on heating and cooling with constant rate 2 K/min. Comparison of $\varepsilon'(T)$ curves for a number of frequencies of the measuring field are shown in Fig. 11(a)–(d) for the ceramics with Bi contents 1, 2, 3, and 4 at.%, respectively. The $\varepsilon'(T)$ characteristics are weakly frequency dependent within the

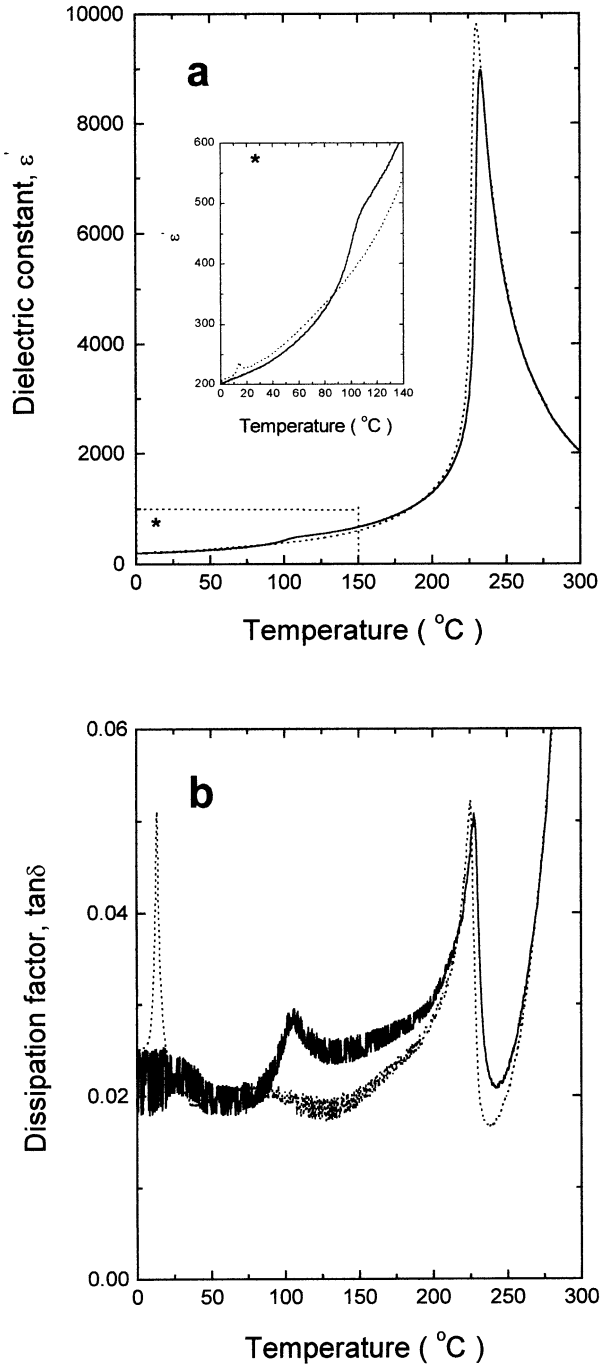

Fig. 10. Dielectric constant (a) and dissipation factor (b) vs temperature on heating (solid lines) and on cooling (dashed lines) for ceramics doped with 2 at.% of Bi.

ranges of A_O and F_R phases. Maxima on the $\varepsilon'(T)$ curves at T_C are, however, frequency dependent, particularly in the case of ceramics with 1 at.% of Bi. In case of this ceramics the maxima in $\varepsilon'(T)$ curves are also twice smaller than in other ceramics. All the studied ceramics show additional maxima in the $\varepsilon'(T)$ curves, observed in the PE phase far beyond the Curie temperature. These additional maxima are higher in the case of ceramics with higher Bi contents and are strongly frequency dependent. With increase in frequency of the measuring field the maxima decrease notably and the corresponding temperatures shift towards higher temperatures. This behaviour is characteristic for relaxors. The plot of natural logarithm of the measuring frequency versus reciprocal absolute temperature, at which dielectric constant attains local minima (in the temperature range $T>$ 300 °C), shows an exponential dependence $f=f_o \exp(-E_a/kT_{min})$, that is in accordance with the Arrhenius formula for the activation energy 0.7–0.8 eV.

6. Electric conductivity

Measurements of electric conductivity versus temperature were carried out in the range of 250–450 °C in order to attain an understanding of the influence of the Bi dopant on the pyroelectric and dielectric characteristics shown above. Weak DC field 10 V/cm was applied to measure the electric conductivity (σ). Examples of the obtained dependence $\ln\sigma$ vs. $1/T$ are shown in Fig. 12(a). The linear character of this dependence made it possible to determine the activation energy of current carriers, 1.4 and 1.2 eV for the Bi-doped and undoped ceramics, respectively.

The effect of the reduction and of the change of the type of electric conductivity was found in the case of the Bi-doped ceramics. This was ascertained by thermoelectric measurements of the Seebeck coefficient (α). The values of this coefficient versus temperature are shown in Fig. 12(b). The Bi- doped ceramics show n-type conductivity whereas for undoped Zr-rich PZT ceramics p-type conductivity is typical.[16]

7. Discussion

The temperatures of structural phase transitions between AFE, FE and PE phases and the wide range in which the intermediate FE phase occurs only weakly depend on the Bi content unlike the La and Nb dopants (Fig. 13 and Table 1). The ceramics with more than 1 at.% of Bi does not show symptoms of an additional phase transition between the two FE phases $F_{R(LT)}$ and $F_{R(HT)}$ as in the case of other ceramics mentioned in Table 1. The role of Bi substitution for Pb ions is most evident in the change of the value and type of electric conductivity (Fig. 12). It is clear that the Bi dopant plays the role of a donor, giving rise to n-type conductivity and its decrease due to the compensation effect. The other substantial difference in the properties of Bi-doped PZT-95/5 ceramics is the exceptional strong broadening of $F_R \rightarrow A_O$ phase transition on cooling and the unusual big effect of its thermal hysteresis (Fig. 3 and 10). It is also striking that on heating the $P_r(T)$

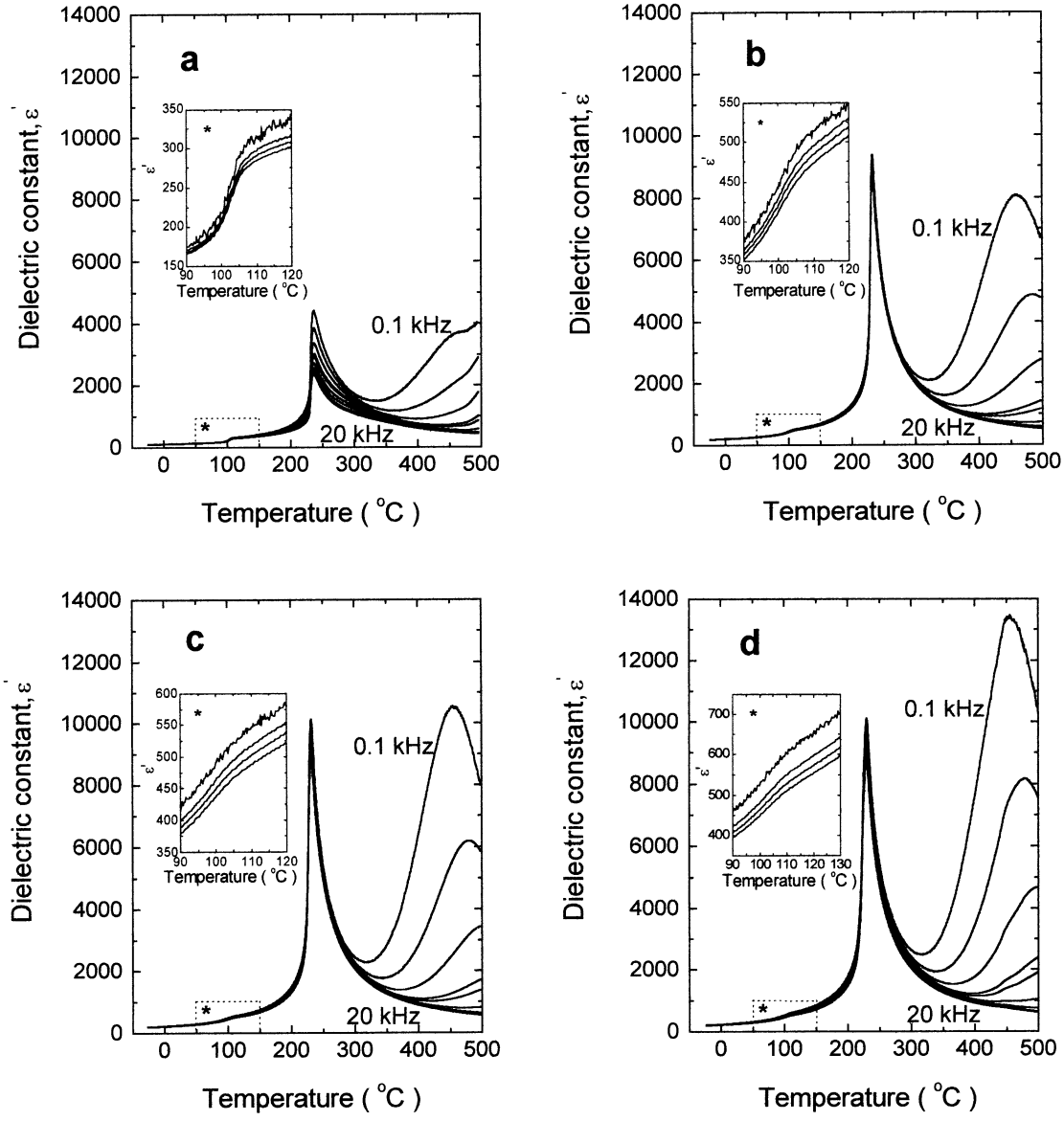

Fig. 11. Dielectric constant as a function of temperature, measured at various frequencies of measuring field for ceramics doped with 1 at.% (a), 2 at.% (b), 3 at.% (c) and 4 at.% (d) of Bi. The individual curves from the top to the bottom concern frequencies: 0.1; 0.2; 0.4; 0.8; 1; 2; 4; 10 and 20 kHz.

curve is relatively steep in case of $A_O \rightarrow F_R$ phase transition (Fig. 3). This means that the expansion of the $P_r(T)$ curve on cooling through $F_R \rightarrow A_O$ transition cannot be interpreted only by compositional fluctuations. The coexistence of neighbouring F_R and A_O phases in a wide temperature range, proved by X-ray measurements[16] and by TEM studies,[10] is probably caused by the effect of a local internal bias field. This is associated with the separation of ion and electron charges, which supports the ferroelectric state, and the associated spontaneous polarisation in some parts of the domains on cooling through the region of $F_R \rightarrow A_O$ phase transition. The field provokes differentiation of local phase transition temperatures and thus a strong broadening and a big effect of the thermal hysteresis of this phase transition is observed. This effect also occurred in other PZT-95/5 ceramics mentioned in Table 1 but it is definitely the strongest in Bi-doped ceramics. In case of PZT-95/5 ceramics the temperature of A_O–F_R phase transition is exceptionally sensitive to the applied DC electric field, as was shown in our paper.[16]

The ion and electron space charges play a much more important role in case of ceramics subjected to a DC electric field prior to the pyroelectric measurements. The pyroelectric effect, and especially this one which occurs in the vicinity of $A_O \leftrightarrow F_R$ phase transitions, strongly depends on the strength of the applied DC field and procedure of the preliminary polarisation of the ceramics. The pyroelectric peak(s) behave entirely differently when the ceramics were pre-poled by the DC field

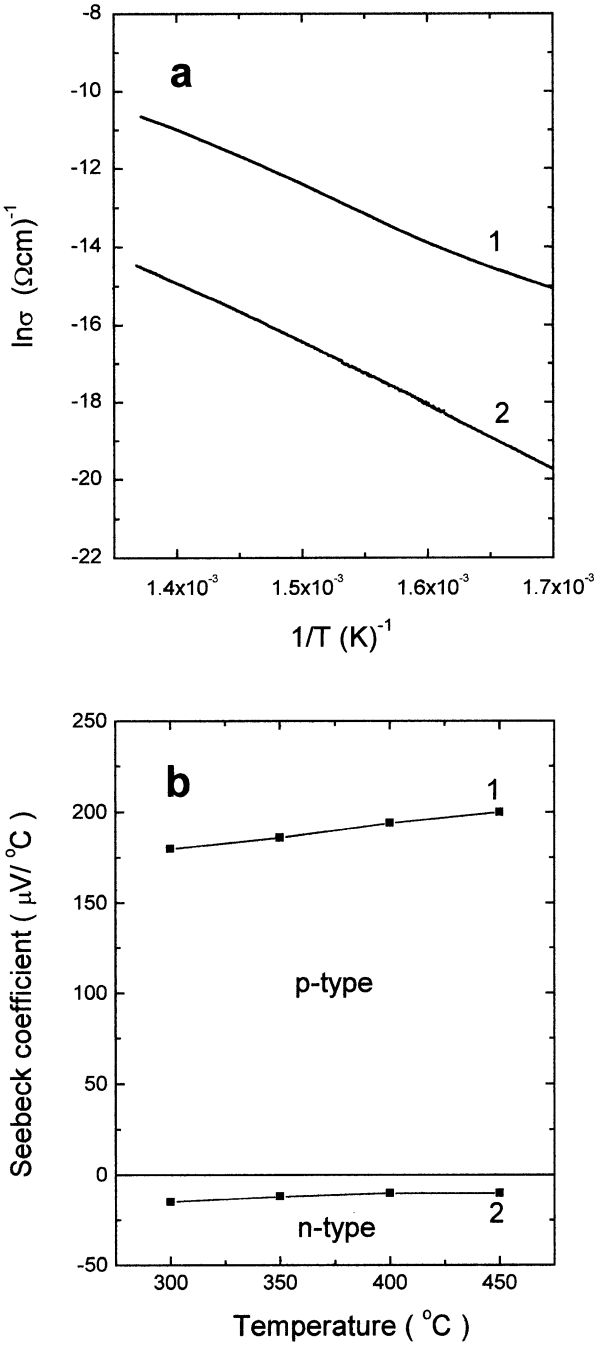

Fig. 12. The electric conductivity vs reciprocal temperature (a) and the Seebeck coefficient vs temperature (b) for ceramics undoped (curves 1) and doped with 2 at.% of Bi (curves 2).

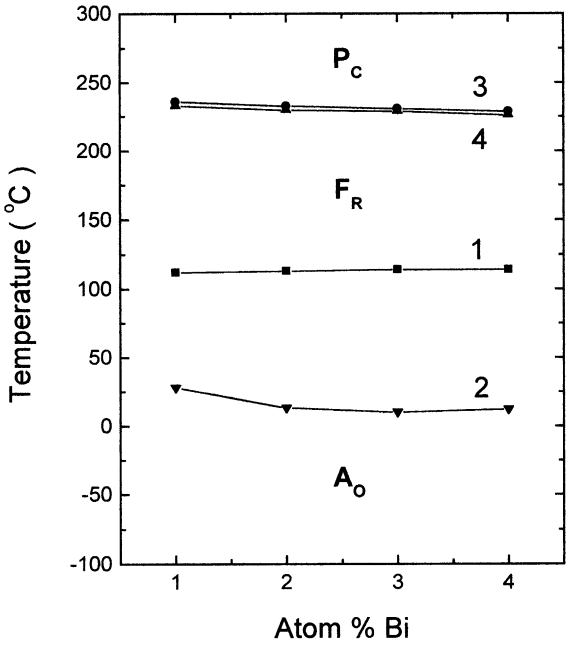

Fig. 13. Variations of A_O–F_R (curves 1 and 2) and F_R–P_C (curves 3 and 4) phase transition temperatures determined from $\epsilon'(T)$ measurements vs Bi content. The curves 1, 3 and 2, 4 relate to heating and cooling, respectively.

applied at temperatures chosen from the PE phase range and then switched off either in the range of FE or AFE phases (Figs. 5–8). Two peaks of pyroelectric current appeared in the region of AFE↔FE phase transitions during subsequent cooling or heating through temperatures of these transitions. One of them appeared at temperatures of $A_O \rightarrow F_R$ and $F_R \rightarrow A_O$ phase transition, determined from dielectric measurements (Fig. 10). Another peak of opposite sign appeared at considerably lower temperatures, which depend on the strength of the applied DC field and on the pre-poling procedure.

The results shown in Fig. 8 clearly prove the effect of the internal bias electric field, associated with the macroscopic metastable space charge polarization[17] which occurs in the ceramics subjected to the pre-poling procedure, preceding pyroelectric measurements. It was shown in our paper[16] that applied external DC field causes strong shift of $F_R \rightarrow A_O$ phase transition temperature with derivative $dT_{AF}/dE \approx 12$ K/kV cm^{-1} for the PZT-95/5 ceramics. A similar role can be attributed to the internal electric field associated with the metastable space charge polarisation. Probably, the additional low temperature pyroelectric peak [Figs. 5, 7(b) and 8], and in particular its shift with the increase of strength of the applied polarising DC field, is caused by this internal field. The measurements carried out do not allow us to determine the symmetry of the induced low temperature FE phase. It may possibly be the low temperature rhombohedral phase ($F_{R(LT)}$), mentioned above.

Behaviour of pyroelectric peaks, accompanied by $F_R \leftrightarrow P_C$ phase transitions is similar for both the pre-poling procedures mentioned above. The spontaneous polarisation vs. temperature, determined from measurements of pyroelectric current and from hysteresis loops is, in this case, in good agreement. The course of $P(T)$ curves, determined in these two ways differs, however, considerably in the range of $F_R \rightarrow A_O$ phase transition (Fig. 9).

Table 1
Comparison of phase transition temperatures determined from dielectric measurements and width of temperature range of FE phase(s) in PZT-95/5 ceramics with various admixtures of contents 2 at.%

Admixture	Temperatures (°C) of the following phase transitions						Width of temperature range of F_R phase		Thermal hysteresis of A_O–$F_{R(LT)}$ phase transition	From Ref.
	A_O–$F_{R(LT)}$		$F_{R(LT)}$–$F_{R(HT)}$		$F_{R(HT)}$–P_c					
	Heating	Cooling	Heating	Cooling	Heating	Cooling	Heating	Cooling		
Pure	100	24	151	141	240	239	140	225	76	12
Bi_2O_3	113	13	–	–	233	230	120	217	100	Present paper
La_2O_3	130	90	160	–	218	216	88	126	40	13, 15
Nb_2O_5	−20	−50	72	70	230	227	250	277	30	14, 15

Local polar micro-regions remaining after the disappearance of P_s at high enough temperatures above T_C, are probably responsible for the additional, frequency dependent and strongly broadened maxima in the $\varepsilon'(T)$ curves, which occur in the range of PE phase (Fig. 11). The effect of low frequency dielectric dispersion and the role of the polar micro-regions in the observed thermally stimulated depolarisation current in the range of PE phase [Figs. 5 and 7(a)] was described in greater detail in our earlier paper concerning La-doped Zr-rich PZT ceramics.[13] The shift of the wide maximum in TSDC, in relation to the temperature at which the ceramics were pre-polarised, results from mutual interaction of the orientation (dipole) part of the metastable polarisation (''heterocharge'') and the polarisation of the free ion and electron space charges, participating in the screening process (''homocharge'').[18]

Acknowledgements

The authors acknowledge Mrs K. Kozerska for her participation in a part of the measurements.

References

1. Shirane, G., Suzuki, K. and Takeda, A., Phase transitions in solid solutions $PbZrO_3$ and $PbTiO_3$ (II) X-ray study. *J. Phys. Soc. Japan*, 1952, **7**, 12.
2. Sawaguchi, E., Ferroelectricity versus antiferroelectricity in the solid solutions of $PbZrO_3$ and $PbTiO_3$. *J. Phys. Soc. Japan*, 1953, **8**, 615.
3. Wentz, J. L. and Kennedy, L. Z., Primary pyroelectric effect in the PZT-95/5 ceramics. *J. Appl. Phys.*, 1964, **35**, 1767.
4. Berlincourt, D., Krugeager, H. H. A. and Jaffe, B., Stability of phases in modified lead zirconate with variation in pressure, electric field, temperature and composition. *J. Phys. Chem. Solids*, 1964, **25**, 659.
5. Jaffe, B., Cook, W. R. and Jaffe, H., *Piezoelectric Ceramics*. Academic Press, London and New York, 1971.
6. Hańderek, J. and Ujma, Z., Dielectric properties of $PbZr_{1-x}Ti_xO_3$ solid solutions with $PbTiO_3$ up to 5%. *Acta Phys. Pol.*, 1977, **A51**, 87.
7. Morozov, E. M., The nature of phase transitions in lead zirconate with small Ti contents. *Fiz. Tverd. Tela*, 1977, **7**, 42.
8. Whatmore, R. W., Clark, R. and Glazer, M., Tricritical behaviour of $PbZr_xTi_{1-x}O_3$ solid solutions. *Solid State Phys.*, 1978, **11**, 3089.
9. Fritz, I. J. and Keck, J. D., Pressure-temperature phase diagrams for several modified lead zirconate ceramics. *J. Phys. Chem. Solids*, 1978, **39**, 1163.
10. Chang, Y. I., A TEM study of crystal and domain structures of Nb-doped 95/5 PZT ceramics. *Appl. Phys. A: Solid and Surfaces*, 1982, **29**, 237.
11. Wang, Y. L., Cheng, Z. M., Sun, Y. Z. and Dai, X. H., Phase transition study of PZT 95/5 ceramics. *Physica B*, 1988, **150**, 168.
12. Hańderek, J. and Ujma, Z., Phase transitions in PZT-95/5 ceramics studied by dielectric and pyroelectric measurements: unusual properties in the vicinity of the antiferroelectric-ferroelectric phase transition. *J. Phys.: Condens. Matter*, 1995, **7**, 1721.
13. Hańderek, J., Ujma, Z., Carabatos-Nedelec, C., Kugel, G. E., Dmytrów, D. and El-Harrad, I., Dielectric, pyroelectric, and thermally stimulated depolarisation current investigations on lead-lanthanum zirconate-titanate-x/95/5 ceramics with La content x = 0.5%-4%. *J. Appl. Phys.*, 1993, **73**, 367.
14. Ujma, Z., Hańderek, J. and Kugel, G. E., Phase transitions in Nb-doped $Pb(Zr_{0.95}Ti_{0.05})O_3$ ceramics investigated by dielectric, pyroelectric and Raman scattering measurements. *Ferroelectrics*, 1997, **198**, 77.
15. El-Harrad, I., Becker, P., Carabatos-Nedelec, C., Hańderek, J., Ujma, Z. and Dmytrów, D., Raman investigation of undoped, niobium-doped and lanthanum-doped lead zirconate-titanate ceramics. *J. Appl. Phys.*, 1995, **78**, 5581.
16. Hańderek, J., Kwapuliński, J., Ujma, Z. and Roleder, K., The influence of an electric field on the DPT in $Pb(Zr_{1-x}Ti_x)O_3$ ($x \leqslant 0.05$). *Ferroelectrics*, 1988, **81**, 253.
17. Okazaki, K., *Ceramic Engineering for Dielectrics*. Tokyo, 1969.
18. Bräunlich, P., ed., *Thermally Stimulated Relaxation in Solids, Topics in Applied Physics, Vol. 37*. Springer, Berlin, 1979.